Study on Microstructure of PET/Nanopowder Composites

Hua Yin, Dingsheng Yu

Key Laboratory of Beijing City on Preparation and Processing of Novel Polymer Materials, College of Material Science and Engineering, Beijing University of Chemical Technology, Beijing 100029, China

Received 14 July 2008; accepted 13 October 2008
DOI 10.1002/app.29876
Published online 19 March 2009 in Wiley InterScience (www.interscience.wiley.com).

ABSTRACT: In this article, the microstructures of polyethylene terephthalate (PET)/nanopowder of butadiene-styrene-vinylpyridine (BSV) rubber, PET/nanocalcium carbonate, and PET/nanoorganoclay as well as the effects of mechanical properties and crystallization on PET were investigated. Scanning electron microscope (SEM) indicated that when the nanoparticles are added into PET, small spheroidicity-shaped particles were seen in the SEM micrographs, and these particles were not nanopowders themselves. The crystallization of PET is improved with the incorporation of proper quantity of nanopowders of BSV and nanoorganoclay. Nanopowders of BSV and organoclay can enhance PET's mechanical properties but not the nanocalcium carbonate. © 2009 Wiley Periodicals, Inc. J Appl Polym Sci 113: 306–315, 2009

Key words: microstructure; nanopowder; PET; crystallization

INTRODUCTION

Polyethylene terephthalate (PET) is a saturated thermoplastic polyester. Compared with other polyesters, PET has several disadvantages such as rigid molecular chain, low T_g(70–80°C), slow crystallizing rate during process, and so on. The incorporation of some addition agents, including organic, inorganic, or some ionomers, can influence the crystallization velocity, microstructure, and properties.[1–6] The scanning electron microscope (SEM) results illuminated that the microstructures of PET/EPDM and PET/MMT are with the various different contents of EPDM and MMT.[7] Glass fiber also has effects on the microstructures of PET.[8] In recent years, more and more researchers are engaged in the study of nanomaterial-modified PET, and most of the nanomaterials are nanoinorganics or organized inorganics such as clay, montmorillonite, and so on.[5–15] To the best of our knowledge, there are no reports on the microstructure of nanoorganic-modified PET. In this article, the properties of PET, containing organic and inorganic powders, were detected, and their microstructures were also depicted by SEM.

EXPERIMENTAL

Materials

PET (viscosity 0.85 dL/g) is manufactured by Yizheng Chemical Fiber Co. (Jiangsu, China). Butadiene-styrene-vinylpyridine (BSV) rubber (VP-701) was purchased from Beijing Research Institute of Chemical Industry (BRICI), SINOPEC; nanocalcium carbonate powder, treated with titanate coupling agent, was purchased from market; nanoorganic clay was provided by the Institute of Chemistry Chinese Academy of Sciences; other agents were purchased from the market.

Sample preparation

Samples of pristine PET, PET/BSV, PET/nanocalcium carbonate, and PET/nanoclay composites were prepared with corotating twin-screw extruder with a screw diameter of 25 mm and a length-to-diameter ratio of 32 : 1. The nanopowders first were dried at 90°C for about 4 h and incorporated into PET, and then fed into the twin-screw extruder. The compounding was carried out at a temperature profile of 234–240–250–255–255–250 from the hopper to the strand die. The extruder's speed was set at 300 rpm.

Test of mechanical properties

The pellets prepared by the extruder were dried in an oven at 100°C for about 6 h and then injection-molded into standard specimens with a temperature profile of 240–255–265–265, mold temperature 65–80°C, and molding time 120 s. Dimensions of the specimens are as follows: tensile specimens were adopted with Type I in ASTM D-638-03; flexural strength/modulus with the dimension length × width × thick ($L \times W \times T$) of 127 × 12.7 × 3.2 (mm^3) and Izod notched impact with $L \times W \times T$ of 63.5 × 12.7 × 6.4. Placed statically for

Correspondence to: D. Yu (yuds@mail.buct.edu.cn).

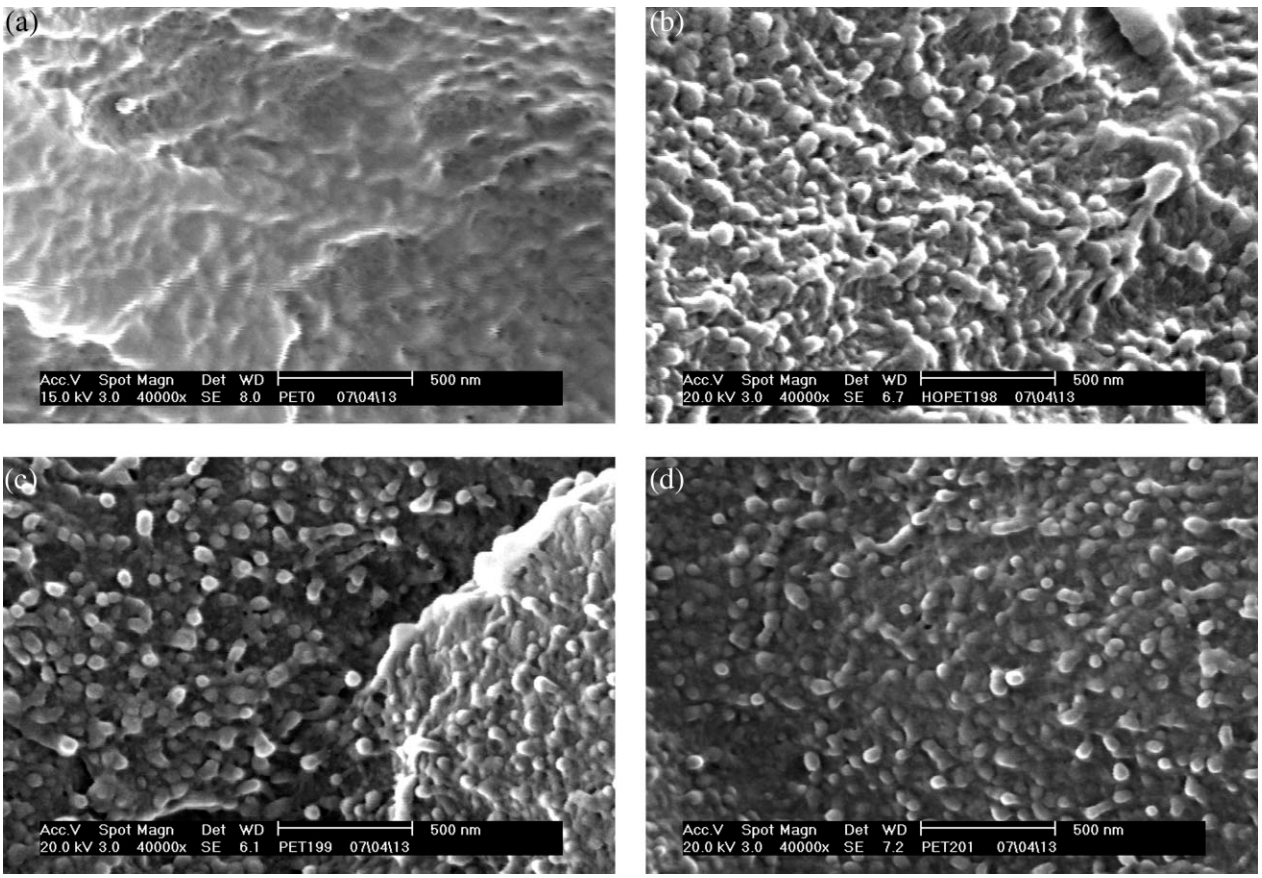

Figure 1 SEM micrographs of PET and PET/BSV: (a) Pure PET, (b) PET/2 wt % BSV,(c) PET/5 wt % BSV, and (d) PET/10 wt % BSV.

about 48 h, the specimens were tested using ASTM method as follows: tensile strength (elongation) with ASTM D-638-03; flexural strength/modulus with ASTM D-790-03; Nothed Izod impact with ASTM D-256-06a. More than five replicate tests were carried out for each mechanical property.

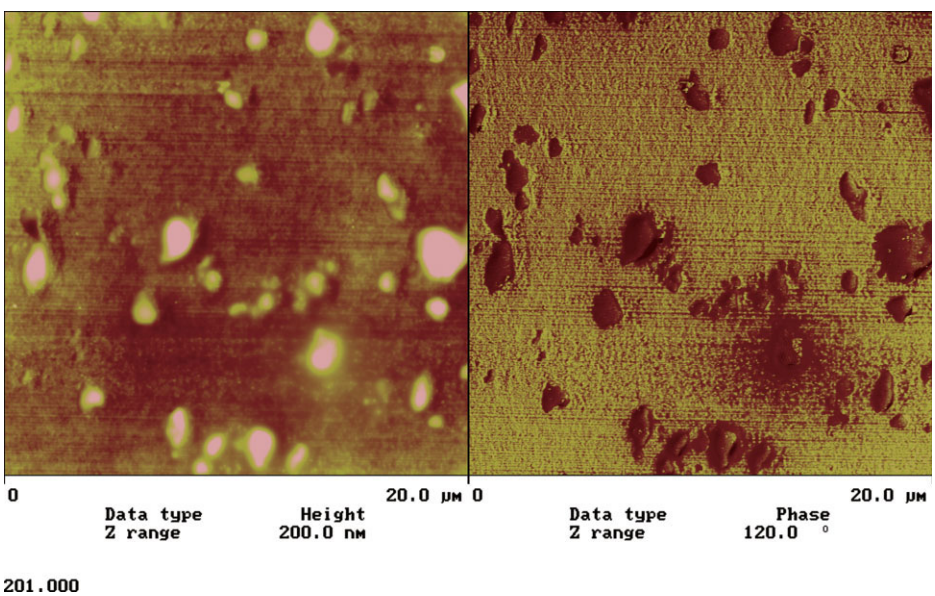

Figure 2 AFM micrographs of PET/BSV. [Color figure can be viewed in the online issue, which is available at www.interscience.wiley.com.]

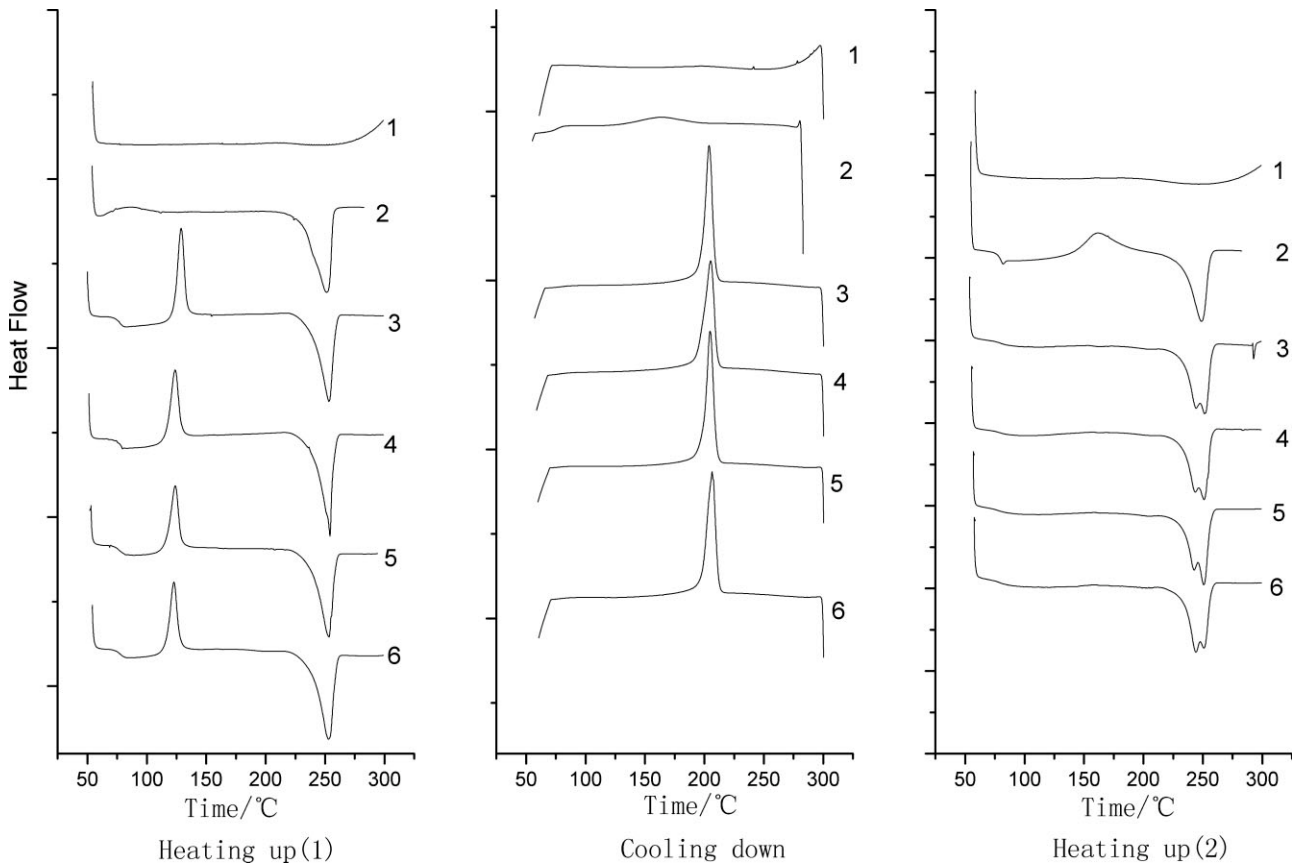

Figure 3 DSC curves for BSV, PET, and PET/BSV. Curves: (1) BSV; (2) Pure PET; (3) PET/2 wt % BSV; (4) PET/5 wt % BSV; (5) PET/7 wt % BSV; and (6) PET/11 wt % BSV.

Scanning electron microscope analysis

The samples were immersed in liquid nitrogen for 20 min and then fractured. The fractured surfaces were coated with gold and then examined by a Phillips XL-30 SEM to observe the microstructures of the samples.

Thermal analysis by differential scanning calorimeter

The analysis was investigated using a Perkin Elmer Diamond differential scanning calorimeter (DSC). The process was as follows: First, the samples were heated up from 40 to 300°C. Then, the melts were

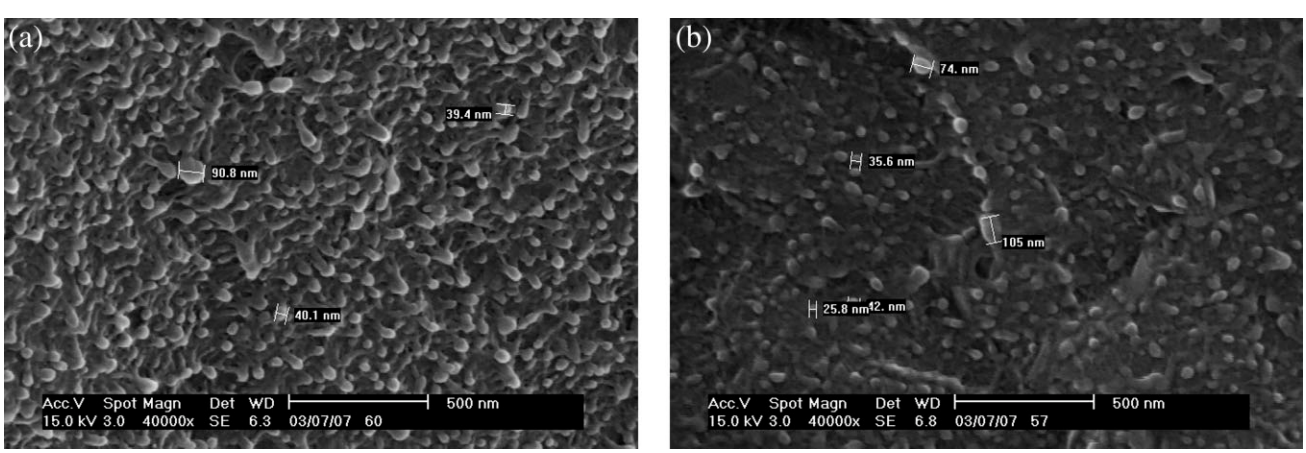

Figure 4 SEM micrographs of (a) PET/nanocalcium carbonate and (b) PET/nanoclay.

TABLE I
Data of PET/BSV Calculated with Jeziorny Method

Crystallinity (%)	Jeziorny method					
		2.5°C/min	5°C/min	10°C/min	20°C/min	40°C/min
	$\ln[-\ln(1 - X_t)]$	$\ln t$	$\ln t$	$\ln t$	$\ln t$	$\ln t$
5	−2.97	1.533	1.352	0.726	−0.124	−0.511
10	−2.25	1.692	1.474	0.861	0.080	−0.265
15	−1.817	1.803	1.561	0.969	0.236	−0.069
20	−1.500	1.912	1.661	1.088	0.427	0.262
25	−1.246	2.069	1.841	1.313	0.868	–

cooled down from 300°C to 40°C. At last, they were again heated up to 300°C. All the process was at a rate of 10°C/min.

RESULTS AND DISCUSSION

The microstructures of PET and PET/butadiene-styrene-vinylpyridine

The microstructures of PET and PET/BSV (2, 5, 10 wt %) were observed through SEM, as shown in Figure 1.

Figure 1 shows the shape like "beach flushed by the sea" in the microscopy of pure PET (SEM) and there are no other crystallites or particles. Micrograph of Figure 1(b) shows the PET containing 2 wt % BSV, it is found that many little irregular ball-like particles, which as if disorderly grew from the matrix, are discovered significantly different from that of pure PET. Figure 1(c,d) shows the micrograph of PET containing 5 and 10 wt % BSV, respectively, in which, many little particles become regular and uniform and densely distribute in the systems with the addition of nano-BSV. These particles size are about 30–60 nm in diameter. However, these particles are not from the BSV added in the PET matrix; is it of some other types? See the following section.

Figure 2 displays the micrograph obtained through a Nanoscope III-a (US Digital Instrument) atomic force microscope (AFM). As described earlier, not more than 10 wt % nano-BSV was added into PET, so BSV is not in a continuous phase, but the PET matrix is in a continuous phase. In the AFM micrographs, the highlighted particles in the height diagram and the deep colored ones in the phase diagram are BSV, that is, discontinuous phase and looks like island. Therefore, little ball-like particles seen in Figure 1 are not BSV but are formed from PET.

DSC analysis for PET/BSV

As illustrated in Figure 3, with the increasing contents of BSV, the peaks of low-temperature crystallizing (cold crystallization) turned into sharp and the values were decreased in heating-up (1) profiles, which indicated the incorporation of BSV improved the crystallization of PET. In heating-up (2) profile, the crystallizing peak of PET without adding BSV is much wider than that of PET with the addition of BSV, which also means that BSV is helpful to the crystallization of PET. In the curves of cooling-down profile, all the crystallizing temperatures are almost at one point. In the second heating-up procedure, the crystalline melts at a point and every peak is separated into two parts (ee heating-up (2) in Fig. 3) and they should belong to different types of crystalline whose melting peak partially overlaps each other. From the SEM micrographs, there are only little ball-like particles distributing in PET, but no evidence proves that whether these particles are crystallites or not. PET crystalline belongs to triclinic system, but these particles are definitely not triclinic. Generally, the addition of BSV is favorable for the crystallization of PET, because BSV can nucleate and its flexibility improves the activity of PET molecular chains.

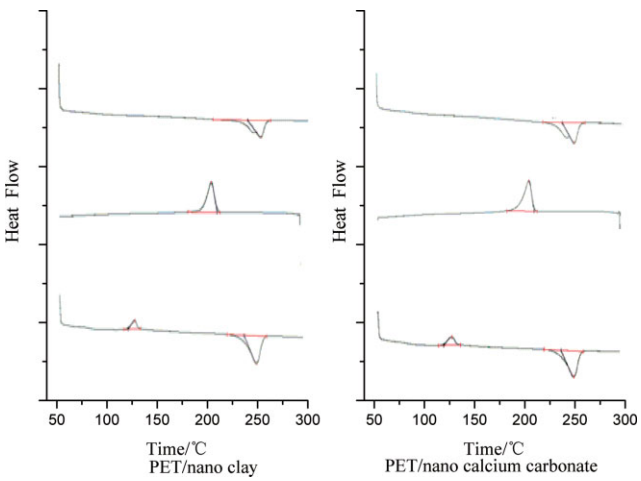

Figure 5 DSC curves for PET/nano calcium carbonate and PET/nanoclay.Curves from up to down in every figure above are separately heating-up, cooling-down, and heating-up (the second time). [Color figure can be viewed in the online issue, which is available at www.interscience.wiley.com.]

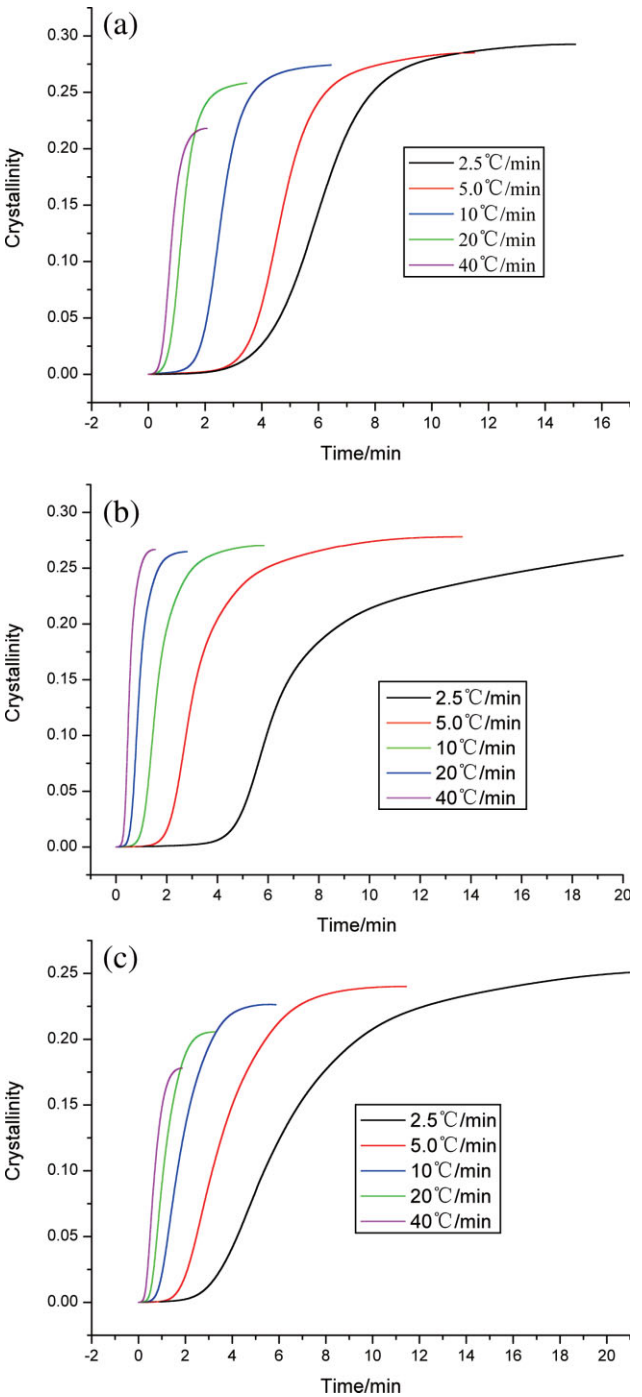

Figure 6 Curves of crystallinity versus time for PET/BSV, PET/nano clay, and PET/nano calcium. Crystallinity versus time for (a) PET/BSV, (b) PET/nano clay, and (c) PET/nanocalcium. [Color figure can be viewed in the online issue, which is available at www.interscience.wiley.com.]

Analysis for PET/nanocalcium carbonate and PET/nanoclay

Figure 4 shows the SEM micrographs of PET/nanocalcium carbonate and PET/nanoclay. After adding the same weight of nanocalcium or nanoclay (4 wt %) into PET, little "ball-like" particles similar to those described in PET/BSV are seen in the picture. From Figure 4, it can be seen that (a) is somewhat different to (b). The little "balls" in (a) protrude outwards hanging down, whereas the "ball" in (b) are immerged in the matrix like cobbles in concrete. Different microstructures between (a) and (b) results in the difference in their properties (see Table I).

DSC analysis for PET/nanocalcium carbonate and PET/nanoclay

Figure 5 shows the DSC curves of PET/nanocalcium carbonate and PET/nanoclay. PET containing 4 wt % nanocalcium carbonate or nanoclay have similar ball-like particles in PET/BSV, from which we can see that the crystallization of the two types of composites are basically similar. The addition of nanocalcium carbonate or nanoclay improved the crystallization. As described earlier, in the second heating-up procedure, there are two peaks overlapping each other, whereas this phenomenon does not appear in the cooling-down procedure. Meanwhile, low-temperature crystallization peak (at about 125°C) appears and this indicate that the effect of nanocalcium carbonate and nanoclay on PET's crystallization is no better than that of BSV's.

Nonisothermal crystallization kinetics of PET

DSC was carried out separately at a series of cooling velocities of 2.5, 5.0, 10, 20, and 40°C/min. Figure 6 shows the relations between the crystallinity and time for PET/BSV, PET/nanoclay, PET/nanocalcium at different cooling velocities. As shown in Figure 6, the crystallinity reached a high value with low cooling velocities, but the crystallization lasted for longer

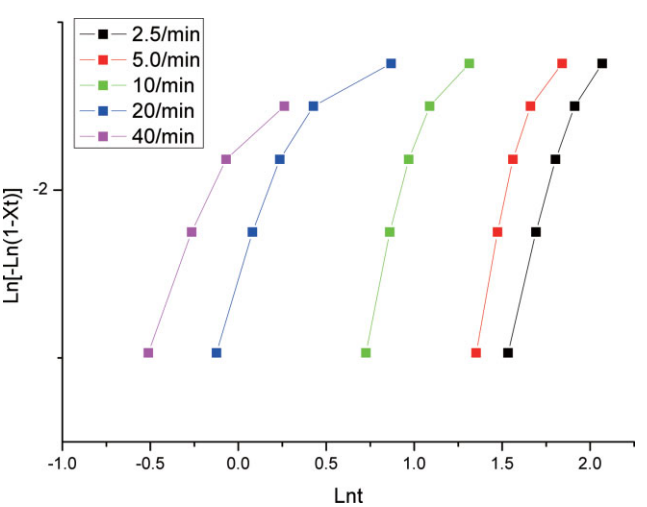

Figure 7 Curves from Table I. [Color figure can be viewed in the online issue, which is available at www.interscience.wiley.com.]

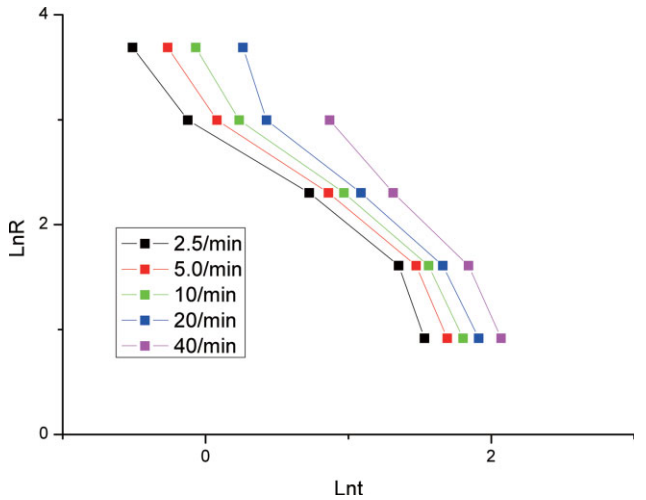

Figure 8 Curves from Table II. [Color figure can be viewed in the online issue, which is available at www.interscience.wiley.com.]

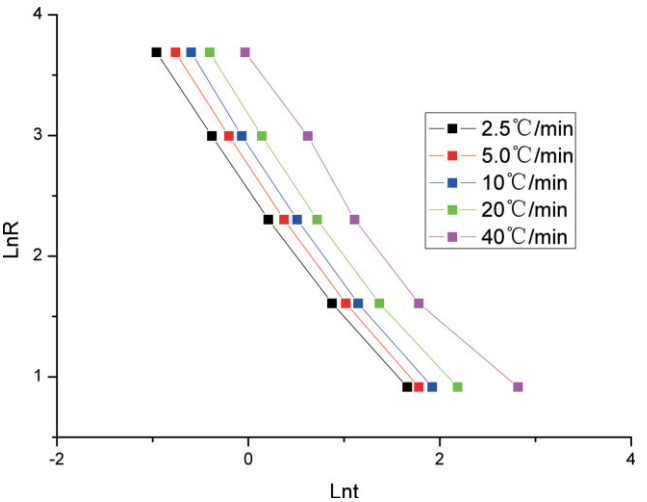

Figure 10 Curves of ln R versus ln t for PET/nanoclay with Mo method. [Color figure can be viewed in the online issue, which is available at www.interscience.wiley.com.]

time. The study of kinetics on these systems was carried out thereafter.

There are some theories about nonisothermal crystallization,[16–19] such as Ozawa, Jeziorny, and Mo method. The three methods are derived from Avrami equation with some modifications. In Ozawa method, Ozawa developed Avrami equation. Nonisothermal crystallization was assumed to consist of infinitesimal isothermal procedure and the equation was worked out as follows:

$$1 - X_t = e^{\frac{K(T)}{R^m}} \tag{1}$$

where $K(T)$ is the function of cooling; R is the cooling velocity; and m is the Ozawa index, which reveals the dimension of crystallization.

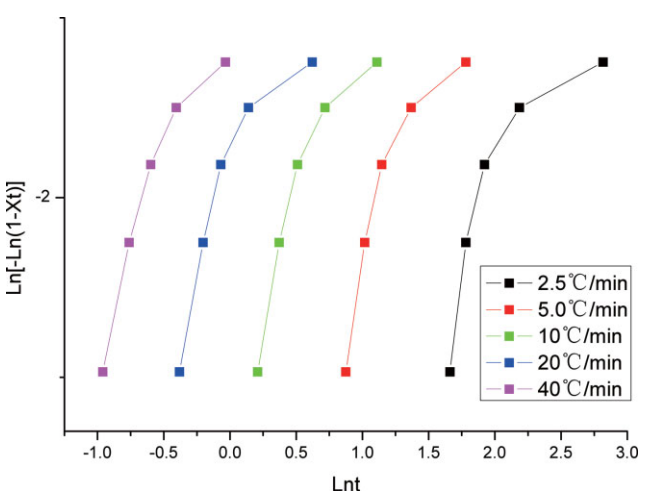

Figure 9 Curves of ln(−ln(1 − X_t)) versus ln t for PET/nanoclay with Jeziorny method. [Color figure can be viewed in the online issue, which is available at www.interscience.wiley.com.]

The Ozawa method had its limitation in dealing with the data obtained in nonisothermal crystallization. Mo combined Ozawa with Avrami equation to work out a new function as follows:

$$\mathrm{lnR} = \mathrm{lnF(T)} - \mathrm{alnt} \tag{2}$$

where $F(T)$ is the cooling velocity needed to get certain crystallinity in unit of time, and $a = n/m$ is the ratio of the index of Avrami and Ozawa.

The Jeziorny method based on the hypothesis of isothermal crystallization came from Avrami equation. This method was actually nonisothermal crystallization as an isothermal procedure, and thereafter some of its parameters were corrected. The following is the function:

$$\ln(-\ln(1 - \mathrm{X_t})) = \mathrm{RlnZ_c} + \mathrm{nlnt} \tag{3}$$

where $Z_t = Z_t/R$.

Jeziorny and Mo theory were used in this work.

As shown in Figure 7 are the plots for ln(−ln(1 − X_t)) vs. ln t. It can be seen that the curves for lower cooling velocities fit linearly better than those for higher velocities with the Jeziorny method; although in general, there are no good linear fitting of ln(−ln(1−X_t)) versus ln t for the PET/BSV system. Figure 8 shows the plot for ln R versus ln t for PET/

TABLE II
Data of PET/BSV with Mo Method

	Mo method[a]				
Cooling rate (°C)	2.5°C/min	5°C/min	10°C/min	20°C/min	40°C/min
ln R	0.916	1.609	2.303	2.996	3.689

[a] All values of ln t are the same as those of Jeziorny method.

TABLE III
Data from Fitting Linear of the Curves in Figure 10

Crystallinity (%)	*A*: intercept	*B*: slope	*F*(*T*)
5	2.6009	−1.06233	13.476
10	2.78584	−1.09478	16.213
15	2.94435	−1.1019	18.998
20	3.1634	−1.07385	23.651
25	3.55029	−0.9907	34.823

BSV, in which, ln *R*s and ln *t*s were not fitting good in the linear relation.

The curves of $\ln(-\ln(1 - X_t))$ versus ln t for PET/nanoclay in Figure 9 indicate that $\ln(-\ln(1 - X_t))$s are not linear with ln *t*s. In Figure 10, the curves are linear lines with Mo method and can well fit the function $y = A + Bx$. Values of A and B are listed in Table III, and the values of $F(T)$, which means the cooling velocities needed to get certain crystallinity in 1 min, were also figured out.

Figures 11 and 12 show the plots of PET/nanocalcium carbonate with the Jeziorny method and Mo method, respectively. The curves ploted with Jeziorny method display no linear relation, which means this method did not fit the function (3). In Figure 12, the curves appear with good linear relationship between ln *R*s and ln *t*s in lower cooling rates (<20°C/min). The data obtained from the fitting curves of Figure 12 are shown in Table IV. Comparing the values of $F(T)$ in Tables III and IV, it can be seen that lower cooling rate was needed in PET/nanoclay than in PET/nanocalcium carbonate to get the same crystallinity.

From this, it can be concluded that the three systems, PET/BSV, PET/nanocalcium carbonate, and PET/nanoclay, have different crystallization behaviors. In PET/BSV, BSV is a kind of high molecular material. Incorporated in PET, BSV affected the PET's crystallization with accelerating the behavior, but in a different way compared with the comparatively low molecular inorganics—nanocalcium carbonate and nanoclay.

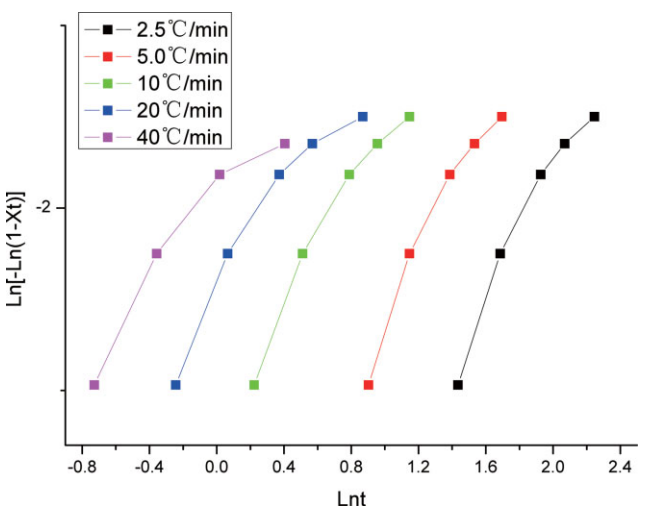

Figure 11 Curves of $\ln(-\ln(1-X_t))$ versus ln t for PET/nanocalcium carbonate with Jeziorny method. [Color figure can be viewed in the online issue, which is available at www.interscience.wiley.com.]

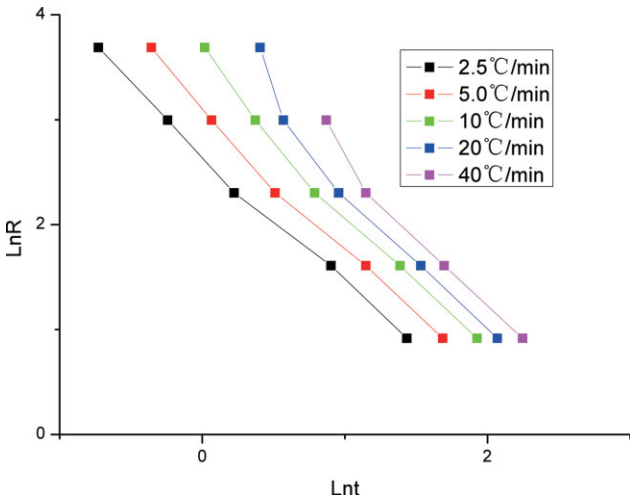

Figure 12 Curves of ln R versus ln t for PET/nanocalcium carbonate with Mo method. [Color figure can be viewed in the online issue, which is available at www.interscience.wiley.com.]

Observation of the microstructure through optical microscope

Figures 13–16 show the micrographs of PET/BSV, PET/nanoclay, PET/nanocalcium carbonate, and PET, respectively. These graphs were observed in a Zeiss Axio Imager A1m phase-contrast microscope (Carle Zeiss) on the samples on a Linkam THMS 600 heating platform at a heating-up and cooling velocity of 5°C/min, with the protection of nitrogen gas. In Graphs (a), of Figures 13–16, optical path difference of the visible light penetrating the sample was converted into amplitude difference, which improved the contrast of all kinds of microstructure. These microstructures of Figure 13(a) apparently differs from that of Figures 14 or 15. The structures in (a) should not be regarded as the micrographs of crystal structure, but the second level of microstructures. It indicates that "the second-level structures" of PET/BSV, PET/nanoclay, and PET/nanocalcium

TABLE IV
Data from Fitting Linear of the Curves in Figure 12

Crystallinity (%)	*A*: intercept	*B*: slope	*F*(*T*)
5	2.7037	−2.6133	14.935
10	3.11623	−1.33295	22.561
15	3.57683	−1.41896	35.76
17.5	4.02458	−1.55638	55.957
20	4.11918	−1.45229	61.509

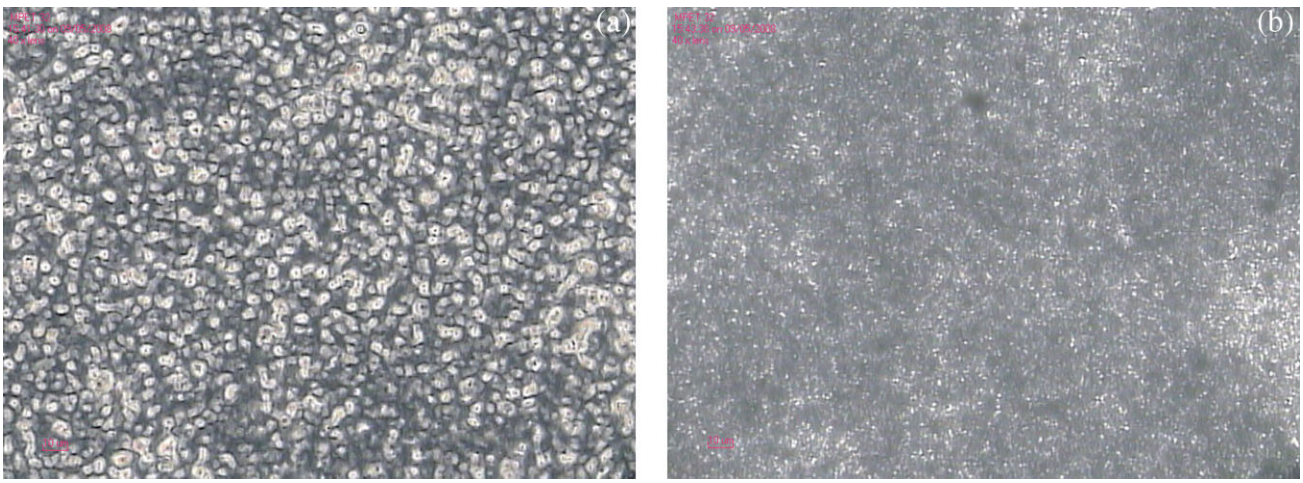

Figure 13 Micrographs of PET/BSV: (a) micrograph of phase contrast and(b) micrograph of crosspolarized light. [Color figure can be viewed in the online issue, which is available at www.interscience.wiley.com.]

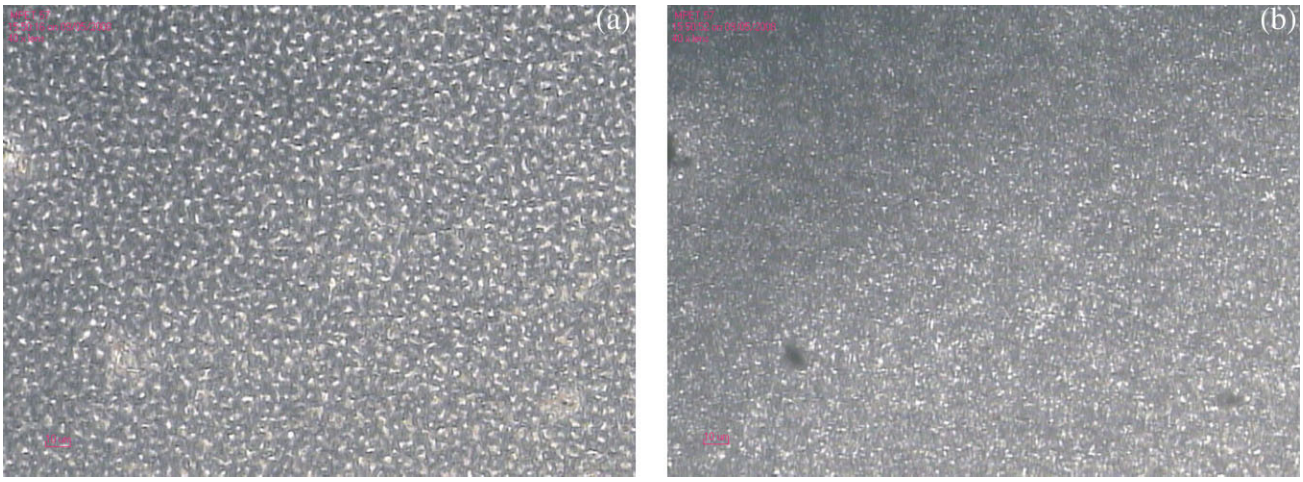

Figure 14 Micrographs of PET/nanoclay: (a) micrograph of phase contrast and (b) micrograph of crosspolarized light. [Color figure can be viewed in the online issue, which is available at www.interscience.wiley.com.]

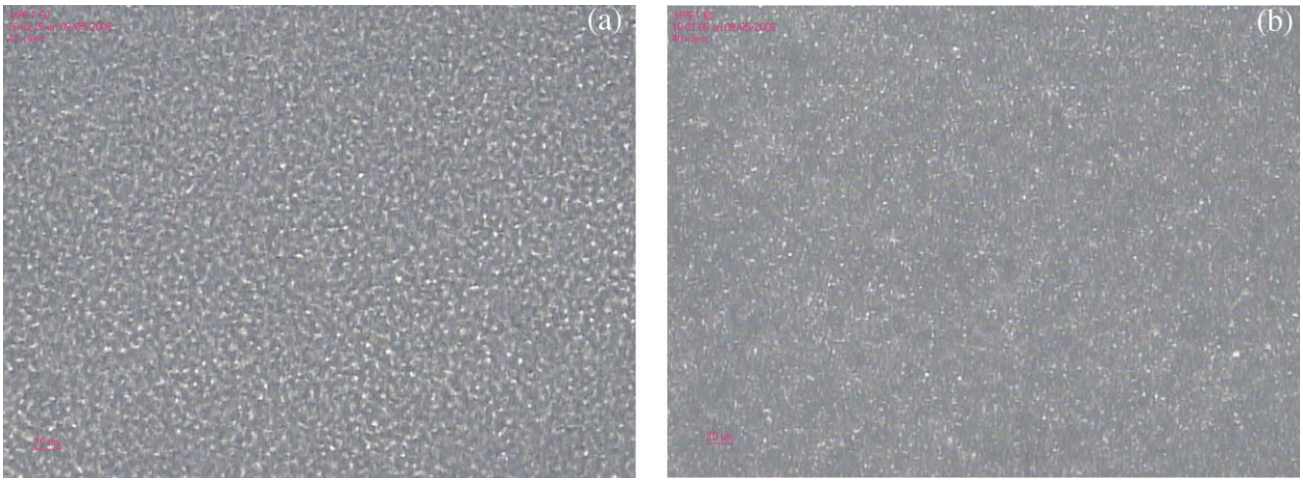

Figure 15 Micrographs of PET/nanocalcium carbonate: (a) micrograph of phase contrast and (b) micrograph of crosspolarized light. [Color figure can be viewed in the online issue, which is available at www.interscience.wiley.com.]

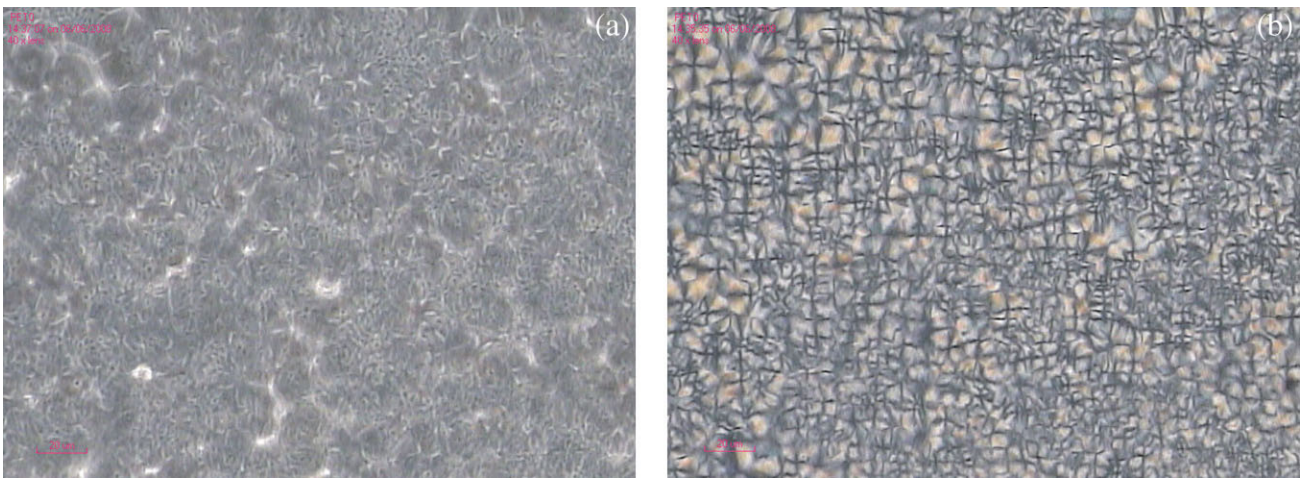

Figure 16 Micrographs of PET: (a) micrograph of phase contrast and (b) micrograph of crosspolarized light. [Color figure can be viewed in the online issue, which is available at www.interscience.wiley.com.]

carbonate are remarkably different from each other. The size of the visible structures in PET/BSV is larger than that in the other systems. This may affect the PET's crystallizing behavior and results in different values in the kinetics of Mo's method for all three systems. The different microstructures leads to their different macroscopical properties.

Figures 13–16 show that the addition of BSV, nanoclay, or nanocalcium carbonate changes PET's microstructure, and the size of crystals in PET get more smaller. Addition of other particles (such as BSV BSV, nanoclay, or nanocalcium) into PET has effects on its cystallinzation, that is, larger number of noncrystalline cores come into being and the space provided for the cores to grow is very limited. The cores' growing speeds are faster, so in shorter time, the crystallites get into shape. At the same time, the growing method of the cores deffer from one another, which results in the distinction of the crystalline and the "second-level structure."

Effects of nanoparticles on properties of PET

Table V displays the properties of PET/BSV, PET/nanoclay, and PET/nanocalcium carbonate with different contents (2, 4, and 6%) of BSV, nanoclay, or nanocalcium carbonate, respectively. Data in Table V indicate that the addition of BSV or nanoclay improves the properties of tensile, flexible, and impact strength. For BSV, its modulus is low, which results in low flexible modulus of PET/BSV; but it contributes to the impact strength because of its own good toughness. According to the theory of Craze-Shear-banding,[20] rubber (BSV) particles play two

TABLE V
Effects of Nanoparticles on PET's Properties

Contents of nanoparticles (%)	Tensile strength (MPa) (±1.4)	Elongation (%) (±1.1)	Flexural strength (MPa) (±1.6)	Flexural modulus (GPa) (±0.06)	Notched Izod impact (J/m) (±2.0)
PET/BSV					
2	57.4	4	94.0	2.56	37.9
4	59.2	5.4	88.1	2.42	39.6
6	55.3	3	82.7	2.28	43.0
8	54.8	6.0	80.5	2.19	54.0
PET/nanoclay					
2	41.9	2.4	81.38	2.92	29.7
4	57.7	4.4	88.00	3.03	37.3
6	55.0	2.4	91.1	3.01	48.1
8	48.8	2.0	88.6	2.90	41.2
PET/nanocalcium carbonate					
2	38.5	2.0	75.74	2.93	16.0
4	43.5	3.0	72.38	2.91	21.3
6	39.4	2.4	54.81	3.25	13.7
8	37.9	2.0	51.7	2.94	13.5
Pure PET					
0	47.6	2.0	85.40	3.12	31.4

important roles: one is, as the focus of stress, to initiate large amount of craze and shear-banding; the other is to control the craze so as to end its extending to prevent resulting in destructive damages. The stress field of the end of craze initiates shear-banding, which holds back further craze extending. Generation of large amounts of craze and shear-banding needs much energy, which is macroscopically indicative of the anti-impact improvement.

Nanoclay is an organic particle and can be better compatible with PET, so the two parts are able to cohere with each other, which leads to the improvement of tensile strength. Nanocalcium carbonate is inorganic particle and incompatible with PET, and therefore, when larger amount of it is added (>2 wt %), the properties of PET/nanocalcium carbonate decline because of bad bonding force between the two phases.

CONCLUSIONS

The BSV incorporated in PET affected the microstructure of PET and many little ball-like particles arise in the system of PET/BSV. These balls are not BSV particles but form due to the effects of BSV, and lightly different with the varying contents of BSV.

In the presence of BSV, the crystallinity of PET has been improved. In the second process of heating-up, there arises double peaks on the melting point, which indicates that they are not identical types of crystalline. Meanwhile, pure BSV's DSC curve has no crystallizing peak, and pure PET's has no double peaks proves that as well.

The addition of nanocalcium carbonate and nanoclay also affects the microstructure of PET and little ball-like particles, which are demonstrated in the SEM of PET/nanocalcium carbonate and PET/nanoclay. These "little balls" in the two systems are different in modalities and there are no larger particles of other types of nonidentical phase discovered. Nanocalcium carbonate and nanoclay are all able to improve the crystallinity, and double peaks appear in their DSC profiles.

Micrograph of phase contrast and crosspolarized light shows the difference of the crystalline and the second-level structure.

Proper amount of nano-BSV or nanoclay reinforces PET's tensile, flexible, and impact strength, whereas nanocalcium carbonate, with its content ratio increasing, deteriorates PET's properties.

References

1. Ajji, A.; Chapleau, N. J Mater Sci 2002, 37, 3893 (in English).
2. Bao, Y.; Huang, Z.; Weng, Z. Suliao Gongye 2004, 32, 21 (in Chinese).
3. Retolaza, A.; Eguiazabal, J. I.; Nazabal, J. J Appl Polym Sci 2003, 87, 1322 (in English).
4. Arencon, D.; Velasco, J. I.; Rodriguez-Perez, M. A.; de Saja, J. A. J Appl Polym Sci 2004, 94, 1841 (in English).
5. Gurmendi, U.; Eguiazabal, J. I.; Nazabal, J. In Proceedings of the Multifunctional Nanocomposites International Conference, Honolulu, HI, US, September 20–22, 2006.
6. Ramanathan, A.; Mallick, P. K. In Proceedings of the 20th Annual Technical Conference of the American Society for Composites; DEStech Publications Inc.: Lancaster, Pennsylvania, 2005; p 138/1 (in English).
7. Li, Y.; Li, Q.-J.; Liang, B.-R. Zhongguo Suliao 2006, 20, 52.
8. Chen, T.; Niu, Y.; Wu, Z. Gongcheng Suliao Yingyong 2006, 34, 29.
9. Li, Z.; Luo, G.; Wei, F.; Huang, Y. Compos Sci Technol 2006, 66, 1022 (in English).
10. Yu, H.-M.; Han, K.-Q.; Yu, M.-H. Cailiao Kexue Yu Gongcheng Xuebao 2005, 23, 537 (in Chinese).
11. Xiao, W.; Yu, H.; Han, K.; Yu, M. J Appl Polym Sci 2005, 96, 2247 (in English).
12. Kint, Darwin, P. R.; Martinez de Ilarduya, A.; Sansalvado, A.; Ferrer, J.; Munoz-Guerra, S. J Appl Polym Sci 2003, 90, 3076. (in English).
13. Sarkissova, M.; Harrats, C.; Groeninckx, G.; Thomas, S. Compos A 2004, 35, 489 (in English).
14. Chang, J.-H.; Kim, S. J.; Joo, Y. L.; Im, S. Polymer 2004, 45, 919 (in English).
15. Rastogi, R.; Vellinga, W. P.; Rastogi, S.; Schick, C.; Meijer, H. E. H. J Polym Sci Part B: Polym Phys 2004, 42, 2092 (in English).
16. Ozawa, T. Polymer 1971, 12, 150.
17. Ziakicki, A. Colloid Polym Sci 1974, 252, 433.
18. Jeziorny, A. Polymer 1978, 19, 11.
19. Mo, Z.h; Liu, J. Gaofenzi Xuebao 1993, 1, 1.
20. Buckmall, C. B. Adv Polym Sci 1978, 27, 121.